Geotech Geol Eng (2024) 42:1611–1622
https://doi.org/10.1007/s10706-023-02634-y

ORIGINAL PAPER

Site Characterisation, Deep Basement Support, Construction, and Deformation Control

Tiyamike Haundi · Horris K. Nangulama · Vincent R. Mbewe

Received: 18 December 2021 / Accepted: 12 June 2023 / Published online: 15 September 2023

Abstract Deep basement construction is characterised by a deformation challenge for the excavation pit and adjacent structures. Basement construction is an unavoidable problem in urban areas. A case is found in a Triumph Unit building block project, where a 14 m basement will be constructed near the existing structures. Conducting a site survey engineering analysis before the deep basement excavation is essential to guarantee safety during basement construction. Site survey engineering analysis is vital in recommending a suitable support structure for the basement pit during excavation. Therefore, this paper takes the Triumph Unit high-rise building basement excavation project as a practical application of site survey engineering analysis on the actual construction site. Geotechnical and groundwater characterisation were achieved through field and laboratory tests. The study revealed that the site was suitable for construction of bored piles as enclosure structure. It also recommended application of steel bracing material enhanced with a hydraulic servo system as basement excavation internal support structure. The recommended support structure is applied to the actual excavation. The excavation-induced deformation with respect to the recommended support structure application is strictly monitored and controlled. The measured project site results show the effectiveness of site survey engineering analysis in recommending a suitable deep basement excavation support system that controls the excavation-induced deformation desirably.

Keywords Site survey engineering analysis · Excavation support · Soft soil excavation · Deformation control

T. Haundi · H. K. Nangulama (✉) · V. R. Mbewe
Department of Mining Engineering, Malawi University of Business and Applied Sciences, Blantyre 312225, Malawi
e-mail: hnangulama@poly.ac.mw

H. K. Nangulama
Research Centre of Coastal and Urban Geotechnical Engineering, Zhejiang University, Hangzhou 310058, China

1 Introduction

As space for urban construction is limited, engineers are using subsurface space for construction (Yihong and Sanfu 2003). Subsurface basement excavation construction redistributes the soil's initial stress (Poulos 2023). Eventually, causing deformation (Wang et al. 2014). The excavation-induced deformation affects the safety of proximity structures (Pawirodikromo 2022; Wang et al. 2014).

Unavoidably, deep basement projects are common in cities with crowded-traffic highways, high-rise buildings, subway metro stations, car parks, etc. (Dong and Jia 2020). In the case of proximity between the basement pit and the adjacent structure,

the basement soil excavation process can cause uneven ground surface settlement, cracks, and structural deformation on the adjacent structure (Guo et al. 2019; Pawirodikromo 2022). To achieve a smooth deep basement construction process in complex urban environments, the site survey engineering analysis is necessary before the basement construction process (Benin et al. 2016).

Many researchers have proved the rationality of carrying out the site survey engineering analysis prior to the commencement of the subsurface basement excavation works (Guo et al. 2019). Researchers such as Nicotera and Valerio (2021), Ni et al. (2021), and Ming-Guang and Demeijer (2020) have pointed out that adequate site survey engineering analysis prior to a deep basement construction causes excellent improvements to the design and construction of urban deep foundation pit basements. Ye et al. (2020) carried out several laboratory tests and field observations to investigate the mechanical and physical characteristics of a project site conditions before a basement construction. They used a 12.8 m Hefei Sheng-li building block basement in Hefei City, China, as a base for site survey engineering analysis. They concluded that the site survey engineering analysis is essential for better selection of the foundation pit support structure that minimises excavation-induced deformation and its associated effects on adjacent structures. Wang (2007) adopted the site survey engineering techniques in a complicated underground construction process. A shield tunnel was to be constructed near the pile groups. The distance of the shield tunnel to the pile groups was 0.80 m. They found that the site survey engineering analysis helped to adopt a deep hole grout reinforcement method that ensured the smooth passage of the shield through the pile groups. Similarly, Ming-Guang and Demeijer (2020) evaluated the site engineering conditions of the Taipei National Enterprise Centre (TNEC) to mitigate the effects of deep basement excavation on existing adjacent structures. They adopted the foundation pit support scheme which the site survey engineering report recommended. They used the finite difference method (FDM) with FLAC 3D, version 5.0 commercial software program. The recommended foundation pit support scheme was numerically modelled to assess its capacity to restrain the excavation-induced deformation impacts on the proximity structures. Their results were consistent with the determinations of Ye et al. (2020) and Wang (2007). Yihong and Sanfu (2003) highlighted that with urbanisation, there are more projects of deep basements adjacent to structures, and the urban land space is getting scarce. The site survey engineering analysis that can help determine deep excavation support structure is a priority for excavation projects in complex environments (Ye et al. 2020; Wang et al. 2014). The present study seeks to extend the understanding of the site survey engineering analysis to the interaction of basement excavation and adjacent structures. This is important in recommending a suitable support system that effectively keeps the excavation-induced deformation within the project's acceptable limits.

In this paper, the Triumph Unit (TU) high-rise building basement excavation project is a practical application of the site survey engineering analysis at the actual construction site. The building block basement excavation project is adjacent to a high-traffic highway, and the high-rise buildings are within the enclave of the basement excavation. The present work demonstrates the effectiveness of site survey engineering analysis to ensure the safety of neighbouring structures and smooth construction of the basement excavation. Based on this analysis, the excavation support system is recommended and applied during the actual excavation works.

2 Site Description and Characterisation

2.1 Project Overview

The actual construction site is a deep foundation pit of Triumph Unit, FG25-R21-18 plot Jing-fang demolition resettlement house, and the west side G1-35B park green space project in Jiang-gang district, Hangzhou City, Zhejiang province, China. The excavation depth for the building block was 14 m. The basement area was 2089.8 m^2, surrounded by a high-traffic highway and high-rise buildings. The west side of the project site is Qiutao high-traffic highway. The high-rise office building block of the China Telecom Jiang-gan branch is on the north side. The south side of the project site is a Hangzhou city Zhonghao building material market. The Sancha new village of high-rise residential building blocks is on the east side of the project site. Figure 1 shows the project construction site together with the monitoring instruments, such

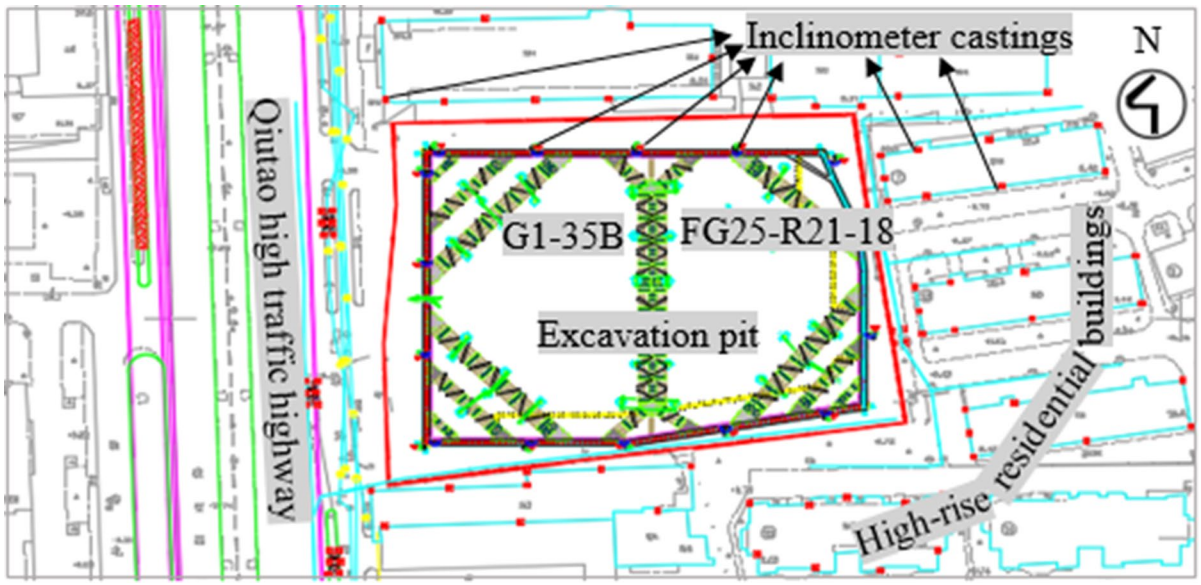

Fig. 1 Triumph Unit project plan view showing the excavation pit, surrounding environment, and the inclinometer points for monitoring purpose

as inclinometers which were placed on surrounding buildings to ensure their safety while the project was being carried out. The various wall lateral displacements and ground movements were monitored to ensure the safety of the project execution.

2.2 Geotechnical Properties of the Site

According to the geological structure background of Hangzhou city and the project site survey geological conditions, no active faults pass through the project area and the surrounding area. The regional structural stability is acceptable. The compression soil layers in the exploration depth are silt, silty, silty clay and the gravel boulder layer. The soil layers' compressibility is from low to high. The foundation site's mechanical properties have minor horizontal and significant vertical differences with consistent uniformity.

The TU building project site belongs to the alluvial plain landform. This means there are no terrain and geological conditions where landslides and debris flow occur. At the time of this analysis, there were no adverse reports of geological effects such as ground subsidence. According to the site survey, the ①1 large layer of miscellaneous fill soil was considered the site's only special soil. The miscellaneous fill soil was distributed in most parts of the site's surface, with a large thickness in the middle and a maximum landfill height of 3.4 m. The miscellaneous filling material was complex, mainly composed of crushed stones, cohesive soil and waste building materials. A small amount of domestic garbage and broken bricks are locally mixed within the fill layer. The filling structure was loose, with poor uniformity and strong permeability. Furthermore, the site consists of underground overhead layers and underground oil tanks of the gas fuelling station, as shown in Fig. 2. The underground overhead layers were the original ventilation foundations of the old residential buildings. Concerning the site survey, the overhead layers and some old local basement residential buildings were used before as storage facilities for some local communities. These areas were identified and levelled.

The drilling and sampling survey method was obtained from the site soil (DB33/T1096 2014). The indoor soil and water tests, such as Atterberg limits, triaxial tests, etc. combined with in-situ test methods such as on-site dynamic penetration test, standard penetration test and single-hole shear wave velocity tests, were conducted on the soil samples. A total of 15 machine drill holes were arranged at the sides and corners of the proposed project basement area to collect soil data across the site. Furthermore, CAD software was used to obtain the coordinates of the hole

Fig. 2 Triumph Unit construction site showing the environmental condition of the site topography and landforms prior to commencement of basement excavation

positioning using the graphical coordinate method (Guo et al. 2019). The coordinates of the exploration points were recorded. The southern "RTK" was used to determine and conduct on-site lofting. The coordinates of the exploration points were derived from GPS control points (Liu et al. 2022). Groundwater characterisation involved collecting samples from two separate drill holes, which were tested for water quality. The results of the water quality analysis are shown in Table 1. The table reveals that the groundwater at the project site is weakly corrosive to the concrete structures. It is slightly corrosive to the steel bars in the reinforced concrete structure under long-term water immersion and slightly corrosive to the steel bar under the alternating dry and wet effects (Alipour and Eslami 2019).

The soil data results within 0–62 m range are quaternary marine and lacustrine deposits alternately deposited in quaternary sea and land phases. The soil at the site is divided into nine sub-layers, as detailed in Table 2. For the stratified statistical results of the physical and mechanical properties of foundation pit site soil, the soil stratum is typical of medium soft silt with silty clayey properties. According to the laboratory test results in Table 3, the groundwater in the exploration depth mainly occurs in ①1 miscellaneous fill soil, ①2 silt, ②1 silty clay, and ②2 sandy silt. The permeability coefficients are relatively small. The dynamic characteristics are climate-regulated. The groundwater level changes seasonally. During the site survey, the measured stable groundwater level in the borehole was 3.14–3.53 m, and the annual change of groundwater level was < 1.5 m. The overlying cohesive soil is a relatively waterproof layer. The top of the aquifer is buried deep, and the permeability is low and partially distributed. The upstream lateral runoff replenishes the aquifer. The upstream lateral runoff is less polluted with evident burial depth and has a high water volume level which varies with the seasons. There were no pressure-bearing water surges observed during the drilling survey. According to the long-term observation data of water near Hangzhou's inner city areas, the aquifer's water elevation (1985 national elevation) is −0.6 to −3.8 m.

Table 1 Triumph Unit project site groundwater corrosiveness to concrete structure and steel bar building materials

Specification	Evaluation of water corrosion to concrete structures					Evaluation of steel bars corrosion in reinforced concrete structures (Alternative dry and wet / long-term water immersion)
	Type II environment			Permeability by formation (Type B)		
	SO_4^{2-} (mg/L)	Mg^{2+} (mg/L)	Total Salinity (mg/L)	PH value	Erosion CO_2 (mg/L)	CL^- (mg/L)
Micro corrosion	< 300	< 2000	< 20,000	> 5.0	< 30	< 100/ < 10,000
Weak corrosive	300–1500	2000–3000	20,000–50,000	5.0–4.0	30–60	100–500/10,000–20,000
Moderately corrosive	1500–3000	3000–4000	50,000–60,000	4.0–3.5	60–100	500–5000/–
Strong corrosive	> 3000	> 4000	> 60,000	< 3.5	–	> 5000/–
Selected borehole 1 groundwater	450	34.74	981.51	7.22	1.90	56.28
Corrosion evaluation	Weak	Micro	Micro	Micro	Micro	Moderate
Selected borehole 2 groundwater	200	22.08	491.84	7.73	1.09	52.73
Corrosion evaluation	Micro	Micro	Micro	Micro	Micro	Moderate

Table 2 Triumph unit project site soil layers' distribution depth, elevation and thickness

Soil layer number	Soil layer name	Buried depth of top soil layer (m)	Floor Top Elevation (m)	Bottom buried depth (m)	Floor top elevation (m)	Soil layer thickness (m)	Soil distribution
		Max–Min	Max–Min	Max–Min	Max–Min	Max–Min	
①1	Miscellaneous fill	0.00–0.00	6.73–6.28	1.80–1.20	5.32–4.61	1.80–1.60	Continuous
①2	Silt	1.50–1.50	5.23–5.03	2.90–2.70	3.88–3.83	1.40–1.20	Local
②1	Silty clay	2.70–1.20	5.32–3.83	3.50–2.90	3.77–2.91	2.00–0.80	Partial
②2	Sandy silt	3.50–2.80	3.88–2.91	13.40–12.60	−5.92 to −6.89	10.40–9.30	Continuous
②3	Silt with sandy silt	13.40–12.60	−5.92 to −6.89	18.80–18.00	−11.52 to −12.39	5.60–5.10	Continuous
⑥	Silty clay	18.80–18.00	−11.52 to −12.39	27.70–26.50	−20.07 to −21.29	9.20–8.10	Continuous
⑦1	Sandy silty clay	27.70–26.50	−20.07 to −21.29	33.50–32.90	−26.19 to −27.09	6.60–5.70	Continuous
⑦2	Cohesive silt sand	33.50–32.90	−26.19 to −27.09	40.70–38.50	−31.97 to −34.29	7.20–5.10	Continuous
⑧	Gravel boulders	40.70–38.50	−31.97 to −34.29	–	–	15.50–8.90	Continuous

The foundation soil structure in the shallow part of the project site is loose. Its uniformity is poor, and its engineering performance is also poor. The site soil structure cannot be used as a natural foundation-bearing layer. The foundation soil at the bottom of the foundation cannot meet the requirements of the main basement foundation pit construction for the bearing capacity of the deep foundation soils (DB33/T1096 2014). The foundation soils exposed in the middle and lower part of the site are cohesive soil and boulders of the gravel layer. The conditions of the foundation soil-bearing layer are analysed as follows:

- ⑥ Layer of silty clay is hard and plastic, the engineering performance is acceptable, the buried depth is shallow, and the bearing capacity is relatively not high. Hence, the layer cannot be considered a bored pile foundation-bearing layer.
- ⑦-1 Layer of sandy, silty clay is soft and plastic; physical and mechanical properties generally deviate. It cannot be considered a bored pile foundation-bearing layer.
- ⑦-2 Silt sand containing cohesive soil, physical and mechanical properties are acceptable. This is because the lower part of it has a better qual-

Table 3 Triumph Unit project site soil layer parameters

Soil layer no	Soil name	Depth (m)	Unit weight γ (kN/m^3)	Cohesion *c* (kPa)	Stiffness Eur (kN/m^2)	Internal friction Angle φ (°)	Poisson ratio	Permeability coefficient K(m/d)
①1	Miscellaneous fill	0–3.4	16.4	4.8	36.42	11.0	0.2	21.4
①2	Silt	3.4–8.1	17.7	11.7	83.24	23.5	0.2	8.8
②1	Silty clay	8.1–19	18.3	15.4	12.8	24.0	0.2	10.2
②2	Sandy silt	19–27	18.9	23.0	79.4	23.3	0.2	5.0
②3	Silt with sandy silt	27–34.2	19.5	23.5	16.8	23.5	0.2	5.7
⑥	Silty clay	34.2–40	19.0	25.8	32.4	30.0	0.2	6.4
⑦1	Sandy silty clay	40–46	19.3	28.5	41.3	15.0	0.2	2.3
⑦2	Cohesive silt sand	46–51.1	18.5	32.0	48.4	21.0	0.2	0.1
⑧	Gravel boulders	51.1–62	21.0	536.0	300.2	34.1	0.3	0.05

ity of gravel boulder layer distribution. It can be considered as a bored pile foundation-bearing layer.

- ⑧ Layer of gravel boulders is mainly medium-density, with high bearing capacity, good engineering performance, continuous distribution, and the layer thickness is 10.9 m deep. The ⑧ layer of gravel boulders is stable according to the site survey and can be used as the bored pile foundation-bearing layer of the main basement.

3 Excavation Support Recommendation

According to the surrounding environment and soil strata analysis of the site, the site is suitable for constructing bored piles as enclosure structures (Dong and Jia 2020). When the pile hole is formed, the protective tube should be buried, and appropriate mud wall protection measures should be adopted (Dong and Jia 2020). The pile hole construction should be feasible. At the same time, there is a need to control the bottom pile hole clearance and the quality of underwater concrete pouring to solve the problem of mud discharge (Hwang 2018). Furthermore, steel bracing material enhanced with a hydraulic servo system is recommended as the basement excavation internal support structure with respect to the protection of the surrounding environment. Hydraulic servo system increases the composite carrying capacity of steel supports during deep excavation (Zhang 2020).

3.1 Earth Retaining Structure

The enclosed bored piles with 600 mm and 800 mm diameters, spaced at 1000 mm (∅600@1000 and ∅800@1000, length 19 m, C35) and high-pressure rotary jet piles as waterproof curtains were used as the excavation pit earth retaining structure. A total of 941 high-pressure rotary jet piles (Φ800@500, length 18 m) surrounded the excavation pit for waterproof sealing, as shown in Fig. 3. The recommended cast-in-place piles are non-squeezed soil piles, and they have less construction noise and vibration (Dong and Jia 2020). As a result, the construction of cast-in-place bored piles at the project site caused little noise and vibration on the surrounding high traffic highway and residential buildings within the enclave of the basement excavation.

3.2 Internal Excavation Support

Three steel bracing levels (with a diameter of 800 mm and thickness of 16 mm steel tube straight support) were used as internal support systems. The steel tube was horizontally spaced 10 m apart at each excavation elevation. The steel bracing vertical spacing was 2.3 m, 4.7 m, and 4.6 m, respectively, as shown in Fig. 3. All three steel bracing supports were preloaded with 1520 kN axial load capacity. The steel bracing internal supports had movable ends for prestress application and were installed at −2.3 m, −7.0 m, and −11.6 m excavation elevations. The steel bracing support at each installation stage (except at −2.3 m elevation) was incorporated with the hydraulic servo

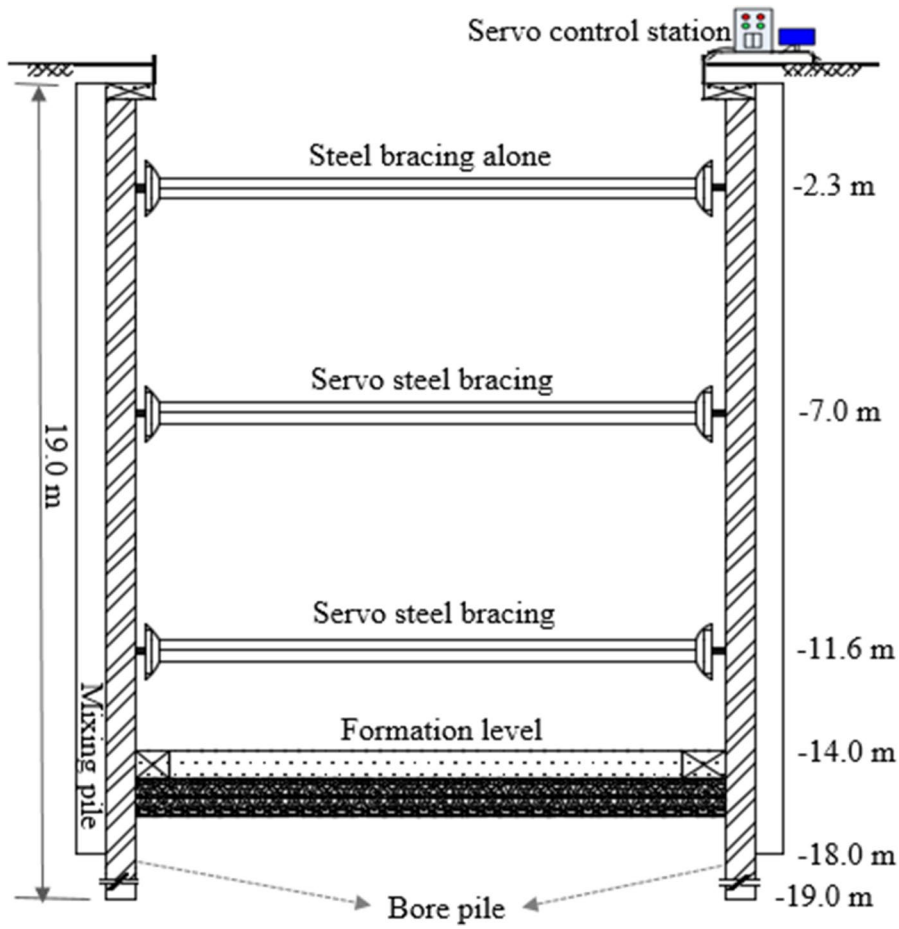

Fig. 3 Triumph Unit building block basement excavation pit support structure cross-section view

system to enhance the steel material lateral support mechanism (Di et al. 2019; Fang et al. 2019; Ming-Guang and Demeijer 2020; Sun 2019).

Different hydraulic servo system axial load capacities were added to the 1520 kN preloaded steel bracing material supporting the excavated pit wall at each installation level during the excavation process. The steel bracing support structure carries loads instantly after installation (Dong and Jia 2020).

4 Excavation Support Monitoring

The project was simulated using the finite element method (FEM) with PLAXIS 3D, version 20.0 commercial software program. The site survey engineering analysis and excavation support recommendations were modelled numerically (Vlachopoulos et al. 2020). Based on the numerical simulation, the maximum excavation-induced displacement was 29.75 mm, as shown in Fig. 4. In this regard, the project's basement construction allowable deformation limits were set. Therefore, the maximum excavation-induced lateral displacement was limited to 0.21% H, where H is an excavation depth of 14 m (14 m, representing 30 mm). The maximum excavation-induced ground surface settlement was not to exceed 0.21% H, and its influence zone was limited to 1.28 H (14 m, representing 18 m) away from the basement excavation edge. This was done for the safety considerations of the adjacent structures, such as the residential building blocks and the Qiutao high-traffic highway, which are 18.07 m and 20.24 m away from the excavation, respectively.

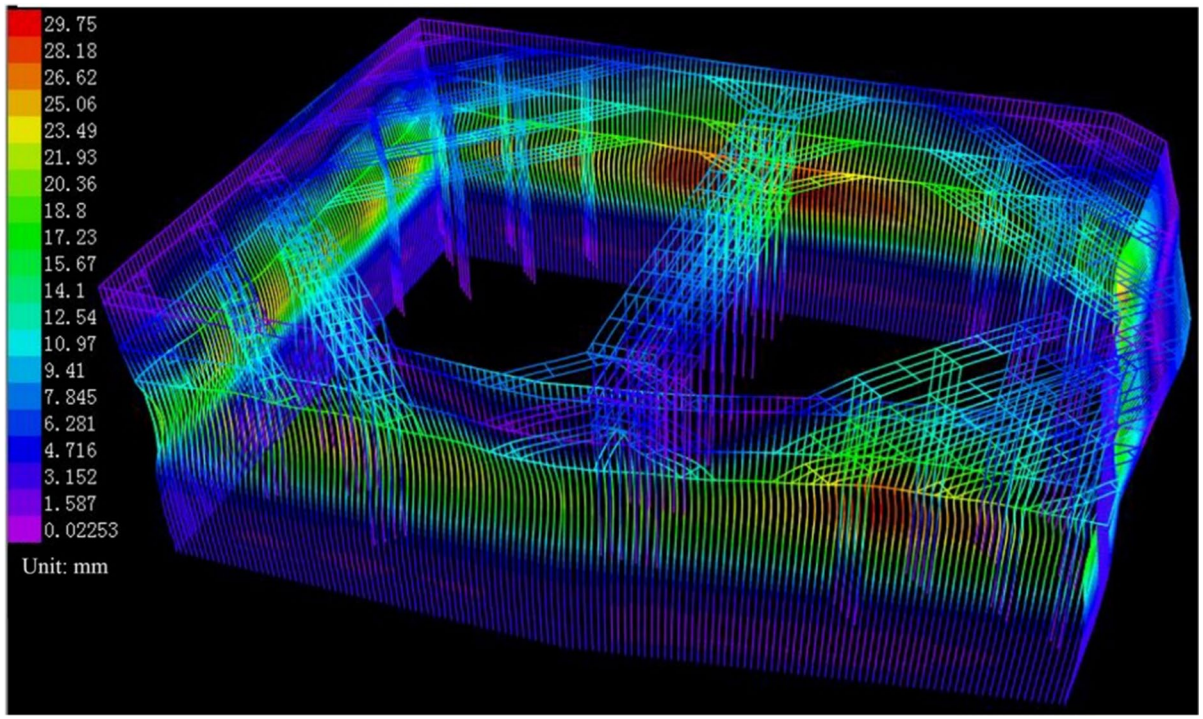

Fig. 4 Simulated three dimension support structure of the recommended Triumph Unit building block basement showing the maximum displacement development profile

4.1 Pile Lateral Displacement

The results were investigated for three different application cases of steel servo-enhanced support structure loading capacity, with the excavation profile unchanged in all three cases. This was done to control the excavation-induced deformation as required.

In the first case, steel bracing with a predefined axial load of 1520 kN was applied in all foundation pit excavation elevations at −2.3 m, −7.0 m, and −11.6 m. The obtained maximum retaining structure pile lateral displacements were 27 mm, 44 mm, and 61 mm at −2.3 m, −7.0 m, and −11.6 m excavation elevations, respectively, as shown in Fig. 5a. The measured pile cumulative lateral displacement meets the limit of 0.21% H (14 m; representing 30 mm) at the −2.3 m stage. As the excavation depth increased, this limit was exceeded. This is confirmed by the results at depths of −7.0 m and −11.6 m.

In the second case, a servo load with 640 kN axial capacity was added at depths of −7.0 m and −11.6 m, where the predefined steel bracing with 1520 kN axial load capacity was installed. In the second case, the total axial load applied at −7.0 m and −11.6 m stages increases to 2160 kN capacity. The predefined steel bracing stiffness with 1520 kN axial load capacity was left unchanged at −2.3 m excavation elevation. Then the retaining structure pile cumulative lateral displacement was again analysed. The measured maximum lateral displacements were 9 mm, 22 mm, and 37 mm for all three elevation stages, as shown in Fig. 5b. The obtained pile cumulative lateral displacement measurement is above the allowable project limit at −11.6 m elevation.

In the third case, the 640 kN servo loading applied at the −11.6 m stage where the displacement incurred exceeds the required limit was adjusted with another servo load of a greater axial load capacity of 860 kN. The servo load with 640 kN capacity was still incorporated at a -7.0 m elevation. The predefined steel bracing with 1520 kN axial loading capacity was maintained in all excavation support elevations. This eventually brings the total support axial load of 1520 kN at −2.3 m stage, 2160 kN at −7.0 m stage, and 2380 kN at −11.6 m stage. After support installation, the measured cumulative lateral displacements were

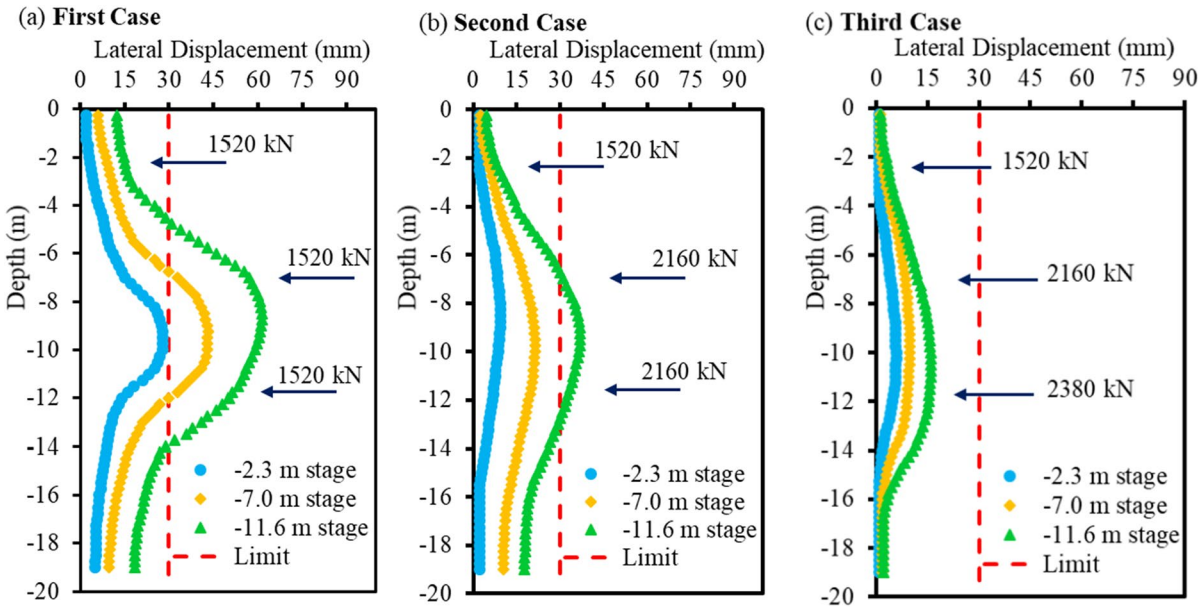

Fig. 5 Triumph Unit building block basement recommended support structure application influence on pile cumulative lateral displacement. **a** Steel bracing alone. **b** 640 kN servo load applied at levels −7.0 m and −11.6 m. **c** 640 kN and 860 kN servo load applied at levels −7.0 m and −11.6 m, respectively

6 mm, 10 mm, and 16 mm at −2.3 m, −7.0 m, and −11.6 m stages, respectively, as shown in Fig. 5c. The maximum cumulative lateral displacement was 0.11% H (14 m; representing 16 mm) at −11.0 m depth when the excavation earthwork was advanced to −11.6 m elevation in the third case. The measurements in the third case are within the required limit of 0.21% H. Compared with the measured maximum lateral displacement in the first case, the pile wall displacement in the third case declined by 74%, 77%, and 78% at −11.6 m, −7.0 m, and −2.3 m excavation stages respectively. Thus, the pile cumulative lateral displacement has reduced by 76% on average with the application of the recommended servo steel enhanced support.

Figure 5 differentiates the measured pile cumulative lateral displacements due to the application of the 1520 kN preloaded steel bracing and different servo axial load capacities in the first case, second case and third case. It can be remarked from Fig. 5 that the pile cumulative lateral displacements obtained in the first case are restrained adequately but not to the extent of meeting the project's allowable limit in all basement excavation stages. The obtained displacement meets the project-required limit at −2.3 m elevation. This finding agrees well with Benin et al. (2016) determination which depicts that the steel support is adequate for lateral support of shallow excavations. When estimated and applied appropriately, steel bracing support in shallow foundations reduces excavation-induced deformation as required (Nicotera and Valerio 2021).

Furthermore, with the incorporation of servo load at −7.0 m in the second case, the retaining structure pile cumulative lateral displacements are further restrained. The measurements are satisfactory for the project's required displacement limit at −2.3 m and −7.0 m elevations but not satisfactory at −11.6 m elevation. With higher servo axial load application at −11.6 m elevation in the third case, the pile cumulative lateral displacements are controlled remarkably to meet the displacement limit. Hence, increasing the applied load in the servo steel bracing helps to limit the retaining structure pile wall displacement induced by the excavation stage. Therefore, the servo steel system placed at a deeper depth optimises the axial load capacity and reduces soil body displacement effectively, as the project site survey requires. The larger the servo steel enhanced the axial load support application in subsequent basement pit elevations,

the greater the pile lateral displacement reduction. This result confirms the effectiveness of the site survey engineering analysis in recommending a suitable foundation pit support system that controls the excavation-induced lateral displacement desirably. Moreover, the measured maximum TU basement excavation-induced displacement satisfies the 0.5% H requirement of soil body displacement limit in the Zhejiang province underground construction project in the inner city of a soft soil environment (DB33/T1096 2014).

4.2 Settlement Influence Zone

Figure 6 shows the measured ground surface settlement profile for the first, second, and third case scenarios. From Fig. 6, the maximum ground surface settlement is 8.5 mm (representing 0.061% H), 6.2 mm (representing 0.044% H), and 2.8 mm (representing 0.020% H) in the first, second and third cases, respectively. In all three cases, the measured maximum ground surface settlement is within the acceptable project displacement limit of 0.21% H (14 m; representing 30 mm). It is noticed that the ground surface settlement increases gradually as the excavation depth increases. Comparatively, the ground surface settlement in the third case reduces by 67% compared to the measured ground surface settlement in the first case when the support was steel bracing without servo. The ground surface settlement declines significantly with higher servo load application in subsequent excavation elevations during the third case. This corroborates well with the determination of Ming-Guang and Demeijer (2020) and Poulos (2023), which shows the effectiveness of the steel servo-enhanced internal support system application on ground surface settlement control.

In addition, during the first case, the ground surface settlement increases with depth. It increases to a maximum value of 8.5 mm at a distance of 8.9 m from the excavation edge when the excavation earthwork is advanced to −11.6 m stage, as shown in Fig. 6a. This confirms that the ground surface settlement increases as excavation depth increases (Charles 2007; Xu et al. 2018; Roboski and Finno 2006). After applying steel support alone, in all excavation elevations in the first case, the ground surface settlement declines rapidly and gets to zero at 22.9 m away from the excavation edge. This finding agrees with the determination of

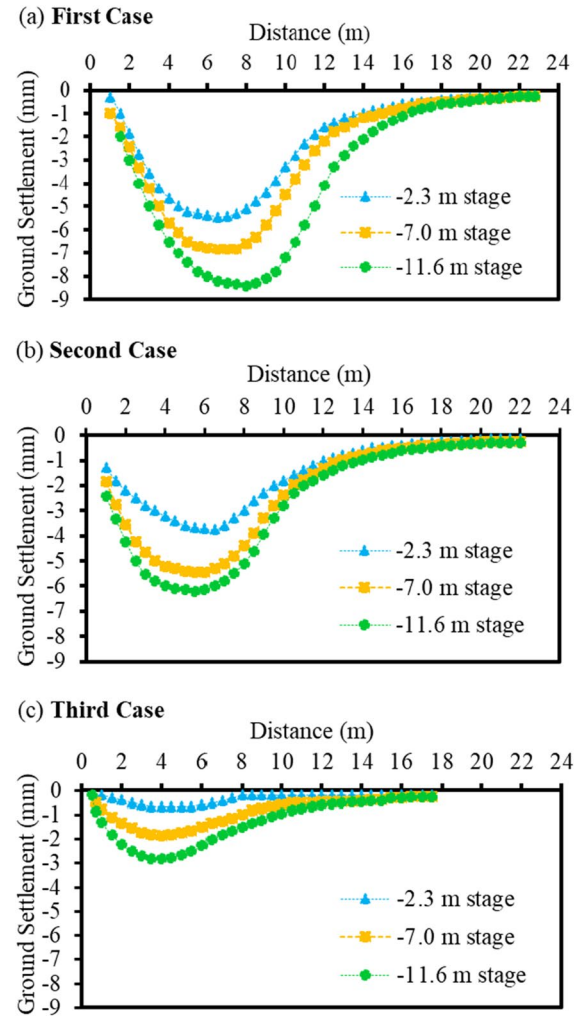

Fig. 6 Triumph Unit building block basement recommended support structure application influence on the profile of ground surface settlement. **a** Steel bracing alone. **b** 640 kN servo load applied at levels −7.0 m and −11.6 m. **c** 640 kN and 860 kN servo load applied at levels −7.0 m and −11.6 m, respectively

Rongzhu et al. (2021), which describes that the steel support alone in an excavation can reduce the ground surface influence zone to a certain degree. However, the measured project ground surface settlement influence zone limit of 1.28 H (14 m; representing 18 m) is exceeded in the first case.

In the second case, the maximum ground surface settlement occurs at 5.0 m during excavation to -11.6 m elevation. It reaches zero at 22.0 m from the excavation edge, as shown in Fig. 6b. Compared with the first case, the ground surface settlement influence

zone reduces by 0.9 m from 22.9 to 22.0 m in the second case. The effect of servo load application at −7.0 m stage in the second case on ground surface settlement influence zone control is unnoticeable and minimal. However, the project required a ground surface settlement influence zone limit of 1.28H (14 m, representing 18 m) is exceeded.

With the application of higher servo load capacity at a subsequent deeper elevation of -11.6 m in the third case, the ground surface settlement influence zone decreases by 5.1 m from 22.9 to 17.8 m (compared with the first case) and by 4.2 m from 22.0 to 17.8 m (compared with the second case). The maximum ground surface settlement occurs at 4.0 m and gets to zero at 17.8 m away from the excavation edge, as presented in Fig. 6c. Moreover, the ground surface settlement influence zone result in the third case is restrained effectively within the acceptable limit of 1.28 H (14 m, representing 18 m). Overwhelmingly, the measured ground surface settlement influence zone in Fig. 6 corroborates well with the proposition by Xu et al. (2018). Xu et al. (2018) highlighted that for deep excavation projects constructed in the inner cities of soft soil environment, the ground surface settlement influence zone should not exceed 3H away from the excavation edge for adjacent structure safety considerations.

5 Conclusion

In this paper, the Triumph Unit high-rise building basement excavation project served as a practical application of site survey engineering analysis on the actual construction site. The soil data was analysed. Geotechnical and groundwater characterisation were achieved through field and laboratory tests. The field tests involved drilling and sampling survey technique, dynamic penetration tests, standard penetration tests, and single-hole shear wave velocity tests. Indoor tests such as atterberg, triaxial tests and water tests were also conducted on the soil samples.

The site survey engineering analysis revealed that the site was suitable for construction of bored piles as enclosure structure. It also recommended application of steel bracing material enhanced with a hydraulic servo system as basement excavation internal support structure. Prior to actual construction works, and for safety of adjacent structures, a finite element method computational PLAXIS 3D software version 20 was used to simulate the recommended support structure. The computer simulation results indicated the maximum excavation-induced displacement of 29.75 mm which gave a base to stipulate the project execution standard on allowable maximum displacement.

With respect to the recommended excavation support application, the induced lateral displacement and ground surface settlement influence zone on actual site were effectively controlled within the stipulated standard. Specifically, the maximum lateral displacement was 16 mm after the basement construction, and the maximum ground surface settlement influence zone was kept under 18 m away from the excavation edge. These findings were within allowable displacements acceptable limits of the project for the safety consideration of the adjacent structures to the deep excavation pit. The measured actual project site results confirm the effectiveness of the site survey engineering analysis in recommending a suitable basement excavation support system that controls the excavation-induced lateral displacement and ground surface settlement distance influence zone desirably.

Funding The authors have not disclosed any funding.

Data availability Enquiries about data availability should be directed to the authors.

Declarations

Conflict of interest The authors reported no potential conflict of interest.

References

Alipour A, Eslami A (2019) Design adaptations in a large and deep urban excavation: case study. J Rock Mech Geotech Eng 11(2):389–399. https://doi.org/10.1016/j.jrmge.2018.08.014

Benin A, Konkov A, Kavkazskiy V, Novikov A, Vatin N (2016) Evaluation of deformations of foundation pit structures and surrounding buildings during the construction of the second scene of the State Academic Mariinsky theatre in saint-petersburg considering stage-by-stage nature of construction process. Procedia Eng 165:1483–1489. https://doi.org/10.1016/j.proeng.2016.11.883

Charles EH (2007) Wall and ground movements associated with deep excavations supported by cast in situ wall in mixed ground conditions. J Geotech Geoenviron Eng 133(2):129–143

DB33/T 1096-2014 (2014) Zhejiang Province construction foundation pit engineering technical specification. China Construction Standards, China (in Chinese)

Di H, Guo H, Zhou S, Chen J, Wen L (2019) Investigation of the axial force compensation and deformation control effect of servo steel struts in a deep foundation pit excavation in soft clay. Adv Civil Eng. https://doi.org/10.1155/2019/5476354

Dong M, Jia P (2020) Stability analysis and parameter optimization of deep excavation supporting system in granular soils. Adv Civ Eng 2020:8873655. https://doi.org/10.1155/2020/8873655

Fang Y, Lu Z, Wang J (2019) Research on safety support technology for ultra-deep foundation pit based on supporting servo combined system. Tunnel Constr 39(Z2):120–128

Guo P, Gong X, Wang Y (2019) Displacement and force analyses of braced structure of deep excavation considering unsymmetrical surcharge effect. Comput Geotech 113(July). https://doi.org/10.1016/j.compgeo.2019.103102

Hwang RN (2018) Effects of preloading of struts on retaining structures in deep excavations. Geotech Eng 49(2):104–114

Liu W, Li T, Wan J (2022) Deformation characteristic of a supported deep excavation system: a case study in red sandstone stratum. Appl Sci (Switzerland), 12(1). https://doi.org/10.3390/app12010129

Ming-Guang L, Demeijer O (2020) Effectiveness of servo struts in controlling excavation-induced wall deflection and ground settlement. Acta Geotechnica

Ni X, Lu J, Wang C, Huang S, Tang D (2021) Systematic analysis method for the unusual large displacement in the excavations in soft soil area. Math Probl Eng 2021:1792089. https://doi.org/10.1155/2021/1792089

Nicotera G, Valerio M (2021) Monitoring a deep excavation in pyroclastic soil and soft rock. Tunnelling and Underground Space Technology, 117:104130. https://doi.org/10.1016/j.Tust.2021.104130

Pawirodikromo W (2022) Ground motions, site amplification and building damage at near source of the 2006 Yogyakarta, Indonesial earthquake. Geotech Geol Eng 40:5781–5798. https://doi.org/10.1007/s10706-02248-9

Poulos HG (2023) Analysis of foundation settlement interaction among multiple high-rise buildings. Geotech Geol Eng 41:2815–2831. https://doi.org/10.1007/s10706-023-02429-1

Roboski J, Finno RJ (2006) Distributions of ground movements parallel to deep excavations in clay. Geotech J. https://doi.org/10.1139/T05-091

Rongzhu L, Jin W, Lianwei S, Wen S (2021) Performances of adjacent metro structures due to zoned excavation of a large-scale basement in soft ground. Tunnell Undergr Space Technol. https://doi.org/10.1016/j.Tust.2021.104123

Sun J (2019) Research on the setting method of the steel support axial force servo system for subway foundation pits. Chin J Undergr Space Eng 15(z1):195–204

Vlachopoulos N, Carrapatoso C, Holt SW (2020) An investigation into support interaction of ground support through numerical modelling and laboratory testing. Geotech Geol Eng 38:5719–5736. https://doi.org/10.1007/s10706-020-01389-0

Wang L (2007) Inspection test and Analysis of axial force in steel brace during construction of Foundation Pit in running tunnel section adjacent to Liming Cultural Club station of Shenyang Metro. Railw Eng 4:86–88

Wang L, Luo Z, Xiao J (2014) Probabilistic inverse analysis of excavation-induced wall and ground responses for assessing damage potential of adjacent buildings. Geotech Geol Eng 32:273–285. https://doi.org/10.1007/s10706-013-9709-4

Xu G, Zhang J, Liu H (2018) Shanghai center project excavation induced ground surface movements and deformations. Front Struct Civ Eng 12(1):26–43

Ye S, Zhao Z, Wang D (2020) Deformation analysis and safety assessment of existing metro tunnels affected by excavation of a foundation pit. Undergr Space (china). https://doi.org/10.1016/j.undsp.2020.06.002

Yihong L, Sanfu YB (2003) Analysis on internal force and deformation of support structure for foundation pit. Chin J Rock Mech Eng 3:462–466

Zhang Q (2020) Deformation analysis of deep foundation pit excavation in China under time–space effect. Geotech Res 7(3):146–152. https://doi.org/10.1680/jgere.20.00009